

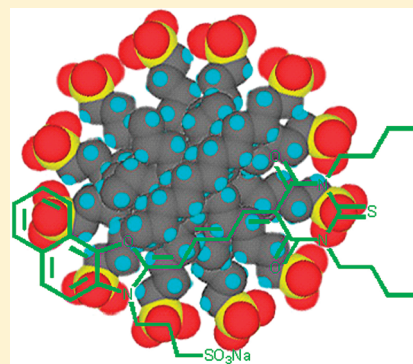
Effect of Pressure on the Solubilization of a Fluorescent Merocyanine Dye by a Nonionic Surfactant

Mohammed A. H. Alamiry, Andrew C. Benniston, and Anthony Harriman*

Molecular Photonics Laboratory, School of Chemistry, Bedson Building, Newcastle University, Newcastle upon Tyne, NE1 7RU, United Kingdom

S Supporting Information

ABSTRACT: The target dye, which is a derivative of Merocyanine 540 bearing a naphthoxazole headgroup, persists as a monomer in ethanol solution but dimerizes in water under ambient conditions. Analysis of the absorption spectrum indicates that the dimer has an oblique geometry with the two molecules being held at an angle of ca. 55° . Applying high pressure to the system forces the two molecules into closer contact, resulting in a decreased partial molar volume of 3.1 cm^3 . One molecule of the monomeric dye enters a neutral micelle formed from Triton X-100, where it is highly fluorescent and free of exciton coupling. The result of applied pressure on these latter systems depends on the concentration of surfactant. Above the critical micelle concentration (CMC), applied pressure has little effect other than to increase the viscosity inside the micelle. At very low surfactant concentration, applied pressure forces monomeric dye into the dimeric form, as observed in the absence of Triton X-100. It is notable, however, that the pressure effect on the dimerization constant is exaggerated in the presence of surfactant. At intermediate surfactant concentrations, applied pressure leads to a marked change in the CMC. In particular, applied pressure reduces the partial molar volume of the micelle by ca. 7.9 cm^3 and induces micelle formation at relatively low concentration of surfactant. For example, the CMC falls from ca. $250 \mu\text{M}$ at atmospheric pressure to only $50 \mu\text{M}$ at 460 MPa.



INTRODUCTION

Surfactants play a major but diverse role in numerous chemical processes and are key components in many important industrial applications.¹ A great variety of surfactants exists, each designed for a particular purpose, although they tend to share common physicochemical properties.^{2,3} Many surfactants are used to generate micelles, which may be charged, neutral or inverse, as a simple means by which to solubilize added solutes.⁴ An essential property of such surfactants relates to the critical micelle concentration (CMC), defined as the concentration of surfactant at which micelles form spontaneously.⁵ Surfactants added to water initially partition toward the interface in order to lower the energy of the interface and to remove the hydrophobic parts of the surfactant from contacts with water. The concentration of surfactant at the surface increases to a maximum before individual surfactant molecules start aggregating into micelles.^{6,7} The opposite situation arises in detergency,^{8,9} where a micellar distribution is disturbed such that the surfactant concentration falls below the CMC. Various techniques can be applied to measure the CMC, including surface tension,¹⁰ viscometry,¹¹ ultracentrifugation,¹² small-angle X-ray scattering,¹³ NMR spectroscopy,¹⁴ conductivity,¹⁵ cyclic voltammetry,¹⁶ gel chromatography,¹⁷ dynamic light scattering,¹⁸ and fluorescence spectroscopy.¹⁹ The latter method is normally based on the use of a dye that is nonfluorescent in water but that emits strongly when dispersed in micellar media. Different strategies can be applied to

render the dye nonemissive in aqueous solution, but the simplest approach requires the dye to be hydrophobic and insoluble in water.

Here we use a derivative of Merocyanine 540, a fluorescent dye widely employed as a probe for membrane polarity,²⁰ as a molecular rotor with which to record the effect of pressure on the self-association of Triton X-100 in water. The latter is a well-known surfactant that forms neutral micelles with a CMC of ca. 0.3 mM under ambient conditions^{21–26} and with an aggregation number of ca. 140.²⁷ The hydrodynamic radius of the resultant micelle is about 70 Å.^{28–30} Triton X-100 has a hydrophilic polyethylene oxide group and a lipophilic hydrocarbon residue, but it is not a single compound (on average it has 9.5 ethylene oxide units in the backbone). For ionic surfactants, it has been shown^{31,32} that the CMC increases with applied pressure, up to about 80 MPa, due to changes in the partial molar volume of the surfactant. As the pressure is increased further, the CMC begins to fall, and at around 250 MPa it returns close to the original value. The reason for this apparent switch in the sign of the pressure-induced change in partial molar volume is not well understood.³³ Less attention has been paid to the effects of applied pressure on the self-association of nonionic surfactants

Received: October 9, 2011

Revised: November 20, 2011

Published: November 22, 2011

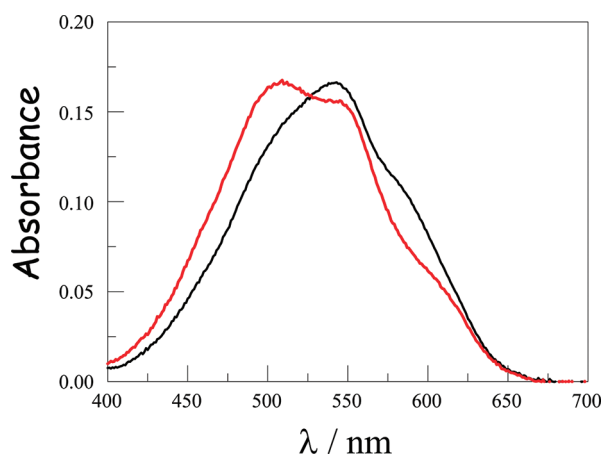


Figure 1. Absorption spectral profiles recorded for BzMC in water at 40 μ M (red curve) and 1 μ M (black curve) in an optical cell of variable path length. See Supporting Information for the full concentration range.

This latter effect is a further consequence of the change in polarizability of the surrounding medium. The increased fluorescence intensity, which occurs without modification of the spectral profile (see Supporting Information), can be corrected for the slight increase in absorbance at the excitation wavelength so as to give the pressure-related Φ_F values. The magnitude of this property increases systematically with increased applied pressure because of the change in microviscosity of ethanol that occurs under these conditions. The overall effect is modest, corresponding to an increase in Φ_F from 0.18 at atmospheric pressure to 0.27 at an applied pressure of 550 MPa. Over this pressure range, there are no obvious indicators for self-aggregation of the solute, but it is clear that BzMC functions as a fluorescent probe for monitoring pressure-induced changes in microviscosity.

Effect of Applied Pressure on the Photophysics in Water.

Despite the presence of the sulfonate group, BzMC does not dissolve readily in water,³⁵ regardless of pH, to give the monomeric species but can be dispersed by sonication to give a stable solution that passes through a 100 nm membrane filter. On varying the total concentration of BzMC present in solution, it becomes apparent that there are two species in equilibrium. The monomeric form of BzMC in water has an absorption maximum at 543 nm, which lies well to the blue of that found in ethanol. Two additional absorption maxima are seen for this solution, these being at 513 and 600 nm, together with isosbestic points at 527 and 553 nm (Figure 1). This behavior suggests that BzMC forms a stable dimer in aqueous solution, as has been concluded for Merocyanine 540.⁴² In fact, going so far as to assume that the associated species is indeed a dimer, it becomes possible to calculate the dimerization constant (K_D) for aqueous solutions by analysis of the observed concentration dependence.⁴³ At a fixed ionic strength of 0.01, K_D has a value of $3.7 \times 10^6 \text{ M}^{-1}$ which can be compared with the value⁴² of $2 \times 10^4 \text{ M}^{-1}$ derived for MC540 in water. This disparity in K_D seems reasonable in view of the larger size of the aromatic nucleus evident for BzMC, which would be expected to favor a higher extent of π -stacking.

The absorption spectrum established for the dimer has pronounced maxima located at either side of the monomer peak. This situation is reminiscent of exciton coupling, which is well-known for cyanine dyes, and the spectral profile can be analyzed in terms of the Kasha model⁴⁴ for an oblique alignment of the

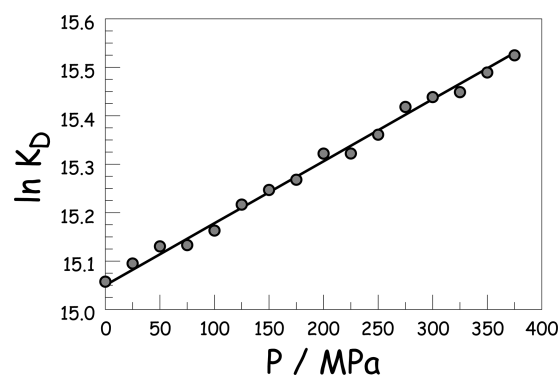


Figure 2. Effect of applied pressure on the dimerization constant derived for BzMC in aqueous solution at 20 $^{\circ}\text{C}$.

respective transition dipoles within the dimer (eq 1). Here, the splitting ($\Delta\nu$) between the two exciton bands is 3000 cm^{-1} while the transition dipole moment for the monomer in water (μ_M) has a value of 9.2 D, as derived from the absorption profile.⁴⁵ Within the model, these data lead to an estimate for the angle (β) between the two chromophores as being 55° . This oblique orientation can be rationalized in terms of computer modeling of the likely geometry for the dimer. The computed structure for the monomer has a relatively high dipole moment of 13.2 D, which arises because of significant contributions from zwitterionic species, and a reasonably flat profile. The thiobarbiturate unit, however, is slightly puckered and electron rich. It is this latter unit, by and large, that prevents parallel stacking between the two BzMC entities.

$$\Delta\nu = \frac{2|\mu_M|^2}{d^3} \left(1 + \cos^2\left[\frac{180 - \beta}{2}\right]\right) \quad (1)$$

$$\left(\frac{\partial \ln K_D}{\partial P}\right)_T = -\frac{\Delta V_M}{RT} \quad (2)$$

The effect of applied pressure is to perturb the equilibrium between monomer and dimer by favoring formation of the latter species, at least at moderate pressure. The measured K_D increases progressively with applied pressure in accordance with eq 2, where ΔV_M is the change in molar volume between dimer and monomer. The results are consistent with ΔV_M taking on a value of -3.1 cm^3 at pressures up to ca. 400 MPa (Figure 2). This overall effect is driven by the need to reduce surface contact between BzMC and the aqueous solvent; the surface area of a single BzMC molecule is computed to be 410 \AA^2 . At higher pressure, K_D remains essentially independent of pressure; absorption spectroscopy shows there is a change in the spectral profile for the dimer but not for the residual monomer. Thus, at pressures exceeding 400 MPa, the exciton splitting of the dimer increases to 3320 cm^{-1} , which must be the result of a pressure-induced change in geometry. It is also apparent that high pressure favors the optical transition into the lower-energy band of the dimer, although the effect is not pronounced. At the highest pressure available to us, which corresponds to 600 MPa, analysis of the absorption spectrum recorded for the dimer shows that the oblique angle is reduced to 45° . As such, we can presume that high pressures cause the two moieties to approach each other more closely and thereby reduce the overall molar volume.

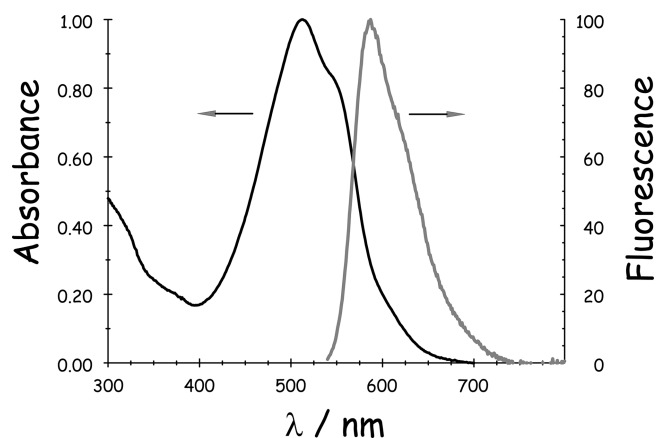


Figure 3. Absorption (black curve) and fluorescence (gray curve) recorded for BzMC in aqueous solution.

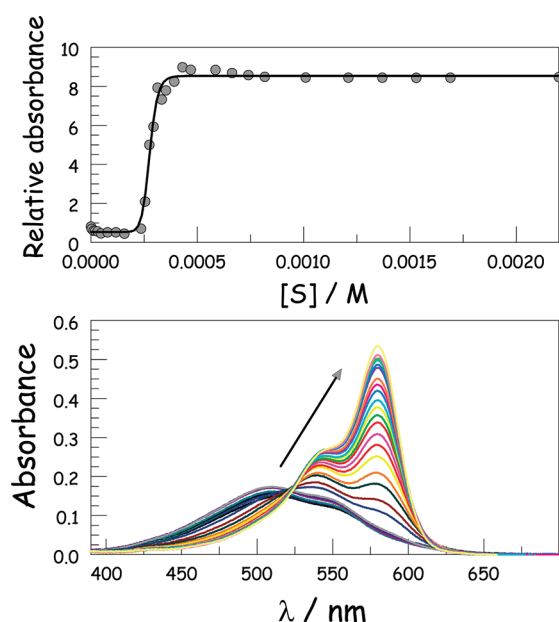


Figure 4. (Lower panel) Evolution of the absorption spectrum recorded for BzMC in aqueous solution during titration with Triton X-100. (Upper panel) Titration curve recorded for the addition of Triton X-100 to BzMC in water. The solid line drawn through the data points corresponds to conventional micelle formation but note the poor fit at the early stage of titration and the overshoot immediately after micelles appear.

In water, BzMC is weakly fluorescent, with the emission maximum appearing at 587 nm (Figure 3). Under these conditions, Φ_F is ca. 0.06 while τ_S has a value of 0.15 ns. This emission can be traced to the monomer species on account of the characteristic excitation spectrum. The dimer does not fluoresce with measurable yield. The fluorescence spectral profile is in reasonable mirror symmetry with the excitation spectrum recorded for the monomer in water. There is a small decrease in the fluorescence yield as the pressure is increased, reflecting the increased tendency to form the dimer at pressures less than 400 MPa. As the pressure is increased above this limit, the fluorescence yield remains constant, in agreement with the pressure-induced effect on K_D . Throughout these pressure-effect studies, there is no change in the fluorescence spectral profile and no

indication for emission from the dimer. This latter finding supports the general idea that only the monomer fluoresces to any real extent in aqueous solution.

Aqueous Surfactant at Atmospheric Pressure. On addition of low concentrations of Triton X-100 ($<100 \mu\text{M}$) to an aqueous solution of BzMC (concentration fixed throughout the study at $4 \mu\text{M}$), the equilibrium between monomer and dimer is pushed very slightly in favor of the monomer (Figure 4). This remains a small effect, however, until reaching a surfactant concentration of ca. $250 \mu\text{M}$. At this point, there is a steep rise in the concentration of a new species that possesses an absorption spectrum resembling that expected for the monomer in an organic solvent; there is a sharp maximum at 579 nm and vibrational satellites stretching toward higher energies. An isosbestic point is preserved at 500 nm during this phase of the titration. At higher concentrations of surfactant, the absorbance at 579 nm tends toward a plateau but, in fact, shows some minor relaxation soon after reaching the maximum absorbance (Figure 4). We can attribute these absorption spectral changes to the solubilization of BzMC by the surfactant, which is able to dissociate the dimer in favor of a surfactant-encapsulated monomeric species. At least three species are needed to fully describe the solubilization process, namely, the monomer (M_F), dimer (D), and the solubilized species (M_M) that most likely corresponds to dye incorporated into a micelle. The spectral changes are inconsistent with the intact dimer being stable in the presence of high concentrations of surfactant.

Upon addition of small amounts of surfactant, the fluorescence yield increases very slightly due to the higher concentration of monomer present under these conditions. Upon reaching a surfactant concentration of ca. $250 \mu\text{M}$, there is a rapid escalation in the fluorescence yield and a shift of the emission maximum to 602 nm. There is little further evolution of the spectral profile or intensity once the surfactant concentration reaches a value of ca. 1 mM (see Supporting Information). Excitation spectra indicate that the species emitting at 602 nm corresponds to M_M . In the plateau region at high surfactant concentration, Φ_F has a value of 0.35 and τ_S is measured as being 0.80 ns. These latter values are reasonably close to those recorded in ethanol under ambient conditions.

Several putative models might be used to account for the effect of surfactant on the optical properties of BzMC in aqueous solution. The simplest model involves self-association of Triton X-100 into micelles, which subsequently extract the dye from aqueous solution. There can be no question of bringing the sulfonate group into the micelle, because of thermodynamic reasoning, and it is highly likely that there will be some structural disturbance around the assimilated dye. At very low concentrations of surfactant, the monomer–dimer equilibrium is shifted slightly in favor of the monomer. This effect is characteristic of the pre-micellar region. As micelles begin to form, the dimer concentration falls and the optical spectra show the coexistence of both M_F and M_M . The inference is that only the monomer enters the micelle and, on this basis, the absorption data collected over a small range of wavelengths can now be analyzed in terms of eq 3 where K_A is the equilibrium constant for uptake of the monomer by the micelle, A_λ is the absorbance at a particular wavelength, while A_0 and A_∞ are the initial and final absorbance values at that wavelength.⁴⁶ From the resultant linear plot, the ratio K_A/N can be determined, where N is the number of monomers contained within a single micelle (see Supporting Information). Now, treating the spectral data in terms of the

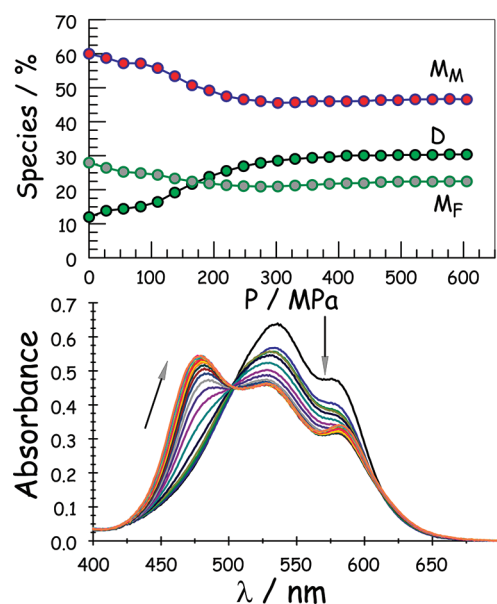


Figure 5. Lower panel: Effect of applied pressure on the fluorescence spectral recorded for BzMC in the presence of Triton X-100 (0.4 mM). Upper panel: Variation of the individual concentrations of dimer, free monomer, and micelle-bound monomer as a function of applied pressure.

Langmuir model,⁴⁷ as outlined in eq 4 where $[D_0]$ and $[M_F]$ refer, respectively, to the concentrations of total dye and free dye in the system while $[M_0]$ is the total micelle concentration, allows separation of these parameters. From this latter analysis, we find K_A has a value of $6 \times 10^5 \text{ M}^{-1}$ while N tends toward unity.

$$A_\lambda - A_0 = A_\infty - A_0 - \left[\frac{K_A}{N} \left(\frac{A_\lambda - A_0}{[M_0]} \right) \right] \quad (3)$$

$$\sigma = \frac{[D_0] - [M_0]}{[M_0]} = \frac{1}{K_A} (N - \sigma) [M_F] \quad (4)$$

On the basis of single occupancy, the effect of added Triton X-100 on the fluorescence properties of BzMC can be analyzed to give a more reliable estimate of K_A (see Supporting Information). Here, the spectral data are consistent with a value for K_A of $8 \times 10^5 \text{ M}^{-1}$, which is in fairly good agreement with that derived from the absorption spectral changes. It might be noted that the concept of single occupancy is in marked contrast to earlier work⁴² carried out with the parent MC540 in sodium dodecylsulfate where it was concluded that up to 10 dye molecules could be accommodated within a single micelle. It might also be noted that fluorescence spectral measurements⁴⁸ have been used to conclude that Triton X-100 binds only a single molecule of 1-anilino-8-naphthalene sulfonate to each micelle, although there are indications for a poorly defined second binding site at high dye concentrations.

Effect of Applied Pressure in the Presence of Surfactant.

Having established that only a single molecule of monomeric BzMC is located in any given micelle, we can now explore the effects of applied pressure on the micellar system. At high concentrations ($>0.5 \text{ mM}$) of Triton X-100, the absorption and fluorescence spectral profiles recorded for BzMC remain unaffected by the application of high pressures ($<550 \text{ MPa}$). In contrast to ethanol, the density of water does not change

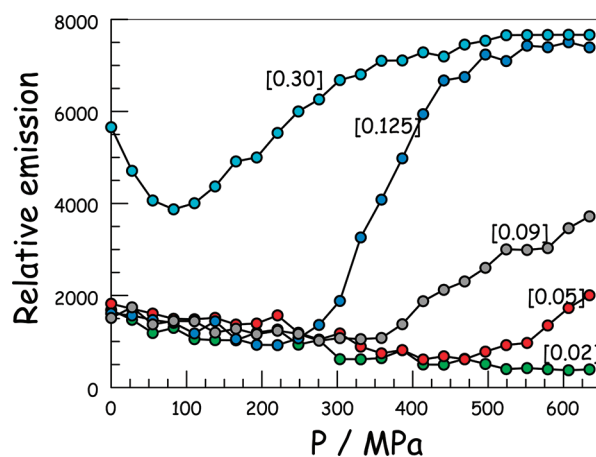


Figure 6. Selected curves showing the effect of applied pressure on the integrated fluorescence signal for BzMC in the presence of different concentrations of Triton X-100. The number shown adjacent to a particular curve is the surfactant concentration (mM).

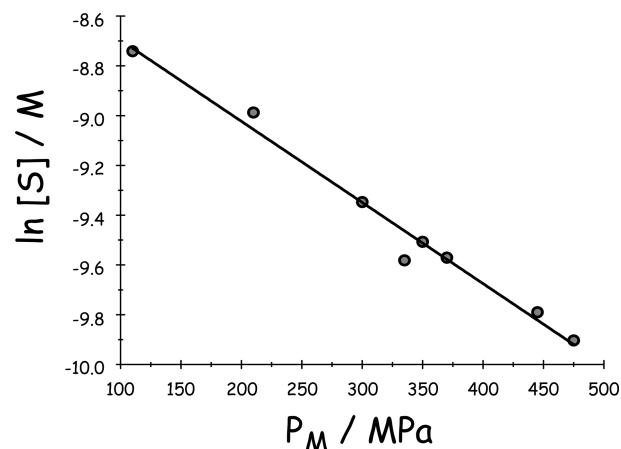


Figure 7. Correlation between the onset pressure, P_M , and the concentration of Triton X-100.

significantly with increased pressure,⁴⁹ so there is little effect on the refractive index or molar volume as the pressure is raised. Under these conditions, BzMC persists as M_M and is relatively fluorescent. Although we might expect that applied pressure will affect the density of any surfactant aggregates present in the system, this has only a small influence on the fluorescence yield. Indeed, there is a continual increase in Φ_F with applied pressure, which approximates to a logarithmic relationship that can be attributed to increased packing of the surfactant around the solute (see Supporting Information). This has the effect of raising the local viscosity, although the effect is small. For a more quantitative understanding, the rate constant (k_{NR}) for nonradiative decay of the excited-singlet state can be calculated from eq 5 on the basis that the radiative rate constant is unaffected by changes in pressure. Here, τ_0 refers to the fluorescence lifetime recorded at atmospheric pressure at surfactant concentrations above the CMC. It is also known⁵⁰ that k_{NR} can be related to viscosity (η) by way of eq 6 where v is a limiting pressure and α is a coefficient that expresses the sensitivity of the system toward changes in bulk viscosity. The remaining term, E_{A_v} represents the activation energy for the viscosity-related nonradiative decay

process; in this case, isomerization of the polymethine backbone. By measuring k_{NR} in a range of alkanols at 22 °C, α has been measured as 0.55. Now, over modest changes in pressure, the so-called Barus equation⁵¹ can be used as a crude measure of how pressure (P) affects viscosity (eq 7), where η_0 is the viscosity at atmospheric pressure. This leads to the general relationship illustrated by way of eq 8, which can be used to describe how changes in pressure affect the internal viscosity for the Triton X-100 micelles. This pressure effect can be expressed in terms of the coefficient χ . Now, for a range of surfactant concentrations above the CMC we find that χ has a common value of 0.0005 MPa⁻¹; that is to say, χ is independent of surfactant concentration over the range 0.5 to 2.5 mM.

$$k_{NR} = \frac{(1 - \Phi_F)}{\tau_0} \quad (5)$$

$$k_{NR} = \frac{v}{\eta^\alpha} e^{-E_A/RT} \quad (6)$$

$$\eta = \eta_0 e^{(\chi P)} \quad (7)$$

$$k_{NR} = \frac{v}{(\eta_0 e^{(\chi P)})^\alpha} e^{-E_A/RT} \quad (8)$$

At surfactant concentrations slightly above the CMC, the system comprises a mixture of D, M_F, and M_M, as can be monitored by absorption spectroscopy. Upon applying pressure to the system, there is a decrease in the absorption bands corresponding to both M_F and M_M and a concomitant increase in absorption due to D (Figure 5). This effect is accompanied by a progressive decrease in fluorescence yield due to the lower concentration of emissive species. An interesting case is found when the surfactant concentration ($[S] = 0.30$ mM) is a little above the CMC (Figure 6). Here, the application of modest pressure ($P < 80$ MPa) causes the loss of fluorescence and the concomitant appearance of M_F and D in the absorption spectrum as noted above. This behavior is consistent with ejection of the dye from the micelle, or with a fall in the micelle concentration. However, the fluorescence starts to reappear at higher pressure ($P > 100$ MPa) while absorption spectroscopy establishes that the dye re-enters the micelle. This behavior is fully reversed upon partial release of the pressure and highly reproducible. The onset pressure (P_M) at which fluorescence recovers, taken from the pressure-fluorescence curves, drops with increasing surfactant concentration whereas the fluorescence yield at the plateau is set by the concentration of dye (Figure 6). The clear inference is that high pressure increases the concentration of micelles, either by reducing the CMC or by lowering the aggregation number. The alternative explanation that two or more dye molecules enter the micelle is inconsistent with the observed shape of the fluorescence–pressure curves. Given the strong dependence between P_M and surfactant concentration, it seems most reasonable to accept that high pressure leads to a reduction in the CMC. Absorption spectral studies carried out under similar conditions remain consistent with this hypothesis.

Turning attention now to very low concentrations of Triton X-100 where micelles are not formed at atmospheric pressure, absorption spectra show an equilibrium mixture of dimer and monomer while the fluorescence spectrum is due solely to the monomer. Progressive increases in pressure force the equilibrium toward the dimer, as expected from Le Chatelier's principle,

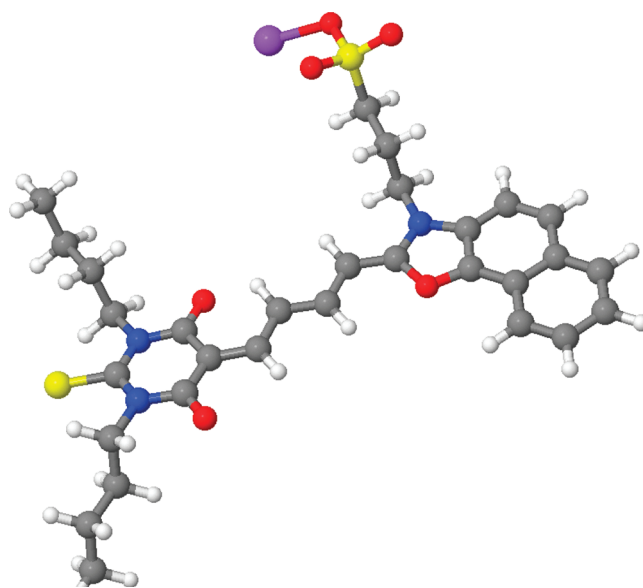


Figure 8. Energy-minimized conformation determined for BzMC in vacuum.

with a concomitant fall in fluorescence intensity. At very low surfactant concentration ($[S] < 70 \mu\text{M}$), the only effect of applied pressure up to 550 MPa is this perturbation of the equilibrium. At atmospheric pressure, K_D decreases in an approximately linear manner as the concentration of Triton X-100 increases, although the effect is small. In the premicellar region, it is notable that the presence of surfactant favors the pressure-induced dimerization step; that is to say, at low concentration of surfactant, K_D is more sensitive toward pressure than in the absence of surfactant, and this sensitivity increases with increasing surfactant concentration. This can be related to the change in molar volume, according to eq 2, which is now a function of surfactant concentration in the premicellar region. The most likely explanation for this unexpected behavior is that surfactant molecules associate with the outermost surface of the dimer and become compressed under pressure.

$$\Delta V_{MC} = RT \left| \frac{\partial \ln \text{CMC}}{\partial P} \right|_T \quad (9)$$

The most reasonable interpretation of these various results is that applied pressure has a marked effect on the CMC of Triton X-100. At high surfactant concentration, any pressure-induced changes in micellar structure remain poorly defined by optical spectroscopy apart from the increase in local viscosity. At low surfactant concentration, the most noticeable spectral changes refer to perturbation of the monomer–dimer equilibrium. It is over the intermediate range, fairly close to the CMC measured at atmospheric pressure, that the most interesting changes occur. Indeed, P_M can be linked to the total surfactant concentration at which fluorescence begins to escalate (Figure 6), and this can be related to the new CMC at that pressure. Now, the effect of pressure on the CMC can be expressed in terms of eq 9, at least over this concentration range. The linear relationship so observed (Figure 7) corresponds to a change in partial molar volume upon the forming the micelle (ΔV_{MC}) of $-7.9 \text{ cm}^3 \text{ mol}^{-1}$. Under these conditions, there is no switch in the sign of the volume change, as reported^{31,32} for the pressure effect on the CMC of other surfactants under very different conditions. Extrapolation of Figure 9 indicates a CMC at atmospheric

pressure of 0.23 mM, which is in the range normally accepted for Triton X-100. Compression of simple alkanes in water is accompanied by a change in partial molar volume⁵² of around $-5 \text{ cm}^3 \text{ mol}^{-1}$, which is similar to the derived value for ΔV_{MIC} . The impression, therefore, is that the pressure effect on Triton X-100 is driven by the need to remove the hydrophobic groups from contact with water. The net result of this effect is that micelles form under high pressure at relatively low concentration; for example, the CMC falls from ca. 280 μM at atmospheric pressure to only 50 μM at 460 MPa. The linearity of Figure 7, taken together with eq 9, permits useful extrapolation of the data to cover a wider pressure range.

CONCLUDING REMARKS

The molecular rotor, BzMC, can be used to monitor aggregation of the neutral surfactant Triton X-100 in aqueous solution and to give a reliable estimate of the CMC. This realization provides an opportunity to explore the effects of applied pressure on the micellar distribution, although it has to be stressed that the rotor will be anchored close to the micelle/water interface and might disrupt the local structure because of its large size. Nonetheless, several interesting features of the pressure effect can be resolved. First, at surfactant concentrations below the CMC, where the probe molecule exists in aqueous solution as a dimer, applied pressure induces solubilization of the dye and thereby favors fluorescence. This behavior is considered to be consistent with a drastic lowering of the CMC at high pressure, but it is difficult to characterize the emergent micelle under these conditions. In particular, it cannot be assumed that the aggregation number remains comparable to that found at atmospheric pressure. This pressure effect is driven by the need to reduce the molar volume, and the simplest way for the system to achieve this goal is to assemble into micelles. Second, unusual behavior is found at surfactant concentrations slightly above the CMC determined at atmospheric pressure (Figure 6). Here, modest pressures cause a reduction in fluorescence intensity, but there is a switchover at higher pressures that results in increased fluorescence. The switchover occurs at 75 MPa for a surfactant concentration of 0.30 mM. In fact, the pressure at which this turnover occurs increases as the surfactant concentration decreases, but the effect occurs only in cases where the probe and micelle concentrations are comparable. We have interpreted the switchover in terms of the probe being ejected from the micelle at modest pressure before re-entering at higher pressure. An alternative explanation involves a pressure-induced change in the number of micelles available to the probe molecule, bearing in mind the single occupancy inherent to this system.

Prior work has reported^{31–33,53,54} similar switchovers in the CMC under applied pressure for various micellar systems, but the underlying reasons are poorly defined. A similar situation is found for the incorporation of nonsurfactant residues, such as long-chain alcohols, into the micellar core.⁵³ Here, an inversion in the CMC-decreasing power of the additive has been noted at pressures of around 120 MPa. In related studies⁵⁵ it has been confirmed that the CMC of Triton X-100 increases with increasing temperature. It is also important to recognize that the probe molecule itself might be subjected to a change in V_{M} at high pressure, thereby complicating the overall picture. For BzMC, the molar volume of the energy-minimized conformer is 522.8 cm^3 (Figure 8). This value could be reduced by compressing the butyl chains attached to the thiobarbiturate unit and by

forcing the propylsulfonate group closer to the polymethine chain. These structural changes are difficult to accommodate with the molecule inside the micelle; in fact, we consider the sulfonate group to act as an anchor that maintains the probe near to the interface. The molar volume for monomeric BzMC is likely to be lower in water than in the micelle because the lipophilic butyl chains will extend in the micellar core, especially because the latter has a fairly open structure near the interface.⁵⁴ Thus, the effects of moderate pressure can be offset by displacing the probe toward the interface. As the pressure increases, the density of the micelle will increase and the probe molecule will become less mobile. The overall molar volume can now be minimized by compressing the surfactant chains, thereby decreasing the CMC, and by encapsulating the probe into the interior.

Finally, the interior of the micelles can be considered to resemble the liquid hydrocarbon state, and it should be noted that Triton X-100 possesses a single phenylene ring that, because of the composition of this surfactant, will be buried deep inside the micelle. There is a small possibility that this aryl group might enter into π, π -stacking interactions with the probe molecule. This possibility seems unlikely, however, since similar spectral shifts were observed in a nonionic surfactant lacking the phenylene ring. Thus, at atmospheric pressure and room temperature, BzMC displays comparable absorption and fluorescence spectral properties in Triton X-100 and Brij 30 micelles. In particular, there are no noticeable shifts to the peak maxima in the two types of microheterogeneous media. Other studies have shown that high pressure can affect the CMC, but there is no obvious theoretical understanding of this effect. With AOT reverse micelles, for example, applied pressure reduces (slightly) the CMC in benzene but causes a substantial increase in the CMC in chloroform.⁵⁶ In other cases,^{53,57} pressure affects the CMC by forcing adventitious substrates into or out of the micelle due to preferential solvation. The nature of the probe molecule, therefore, might play a significant role in establishing how the CMC responds to changes in applied pressure.

ASSOCIATED CONTENT

S Supporting Information. Absorption/fluorescence spectral data for BzMC in ethanol solution at atmospheric and applied pressures, fits to Langmuir and Scatchard models, and fluorescence titration to measure association constant. This material is available free of charge via the Internet at <http://pubs.acs.org>.

AUTHOR INFORMATION

Corresponding Author

*Tel and Fax: +44 191 222 8660. E-mail: anthony.harriman@ncl.ac.uk

ACKNOWLEDGMENT

We thank EPSRC (EP/E014062/1) and Newcastle University for their financial support of this work.

REFERENCES

- (1) Flick, E. W., Ed. *Industrial Surfactants*, 2nd ed.; Noyes Publications: Park Ridge, NJ, 2001.
- (2) Schramm, L. L., Ed. *Surfactants: Fundamentals and Applications in the Petroleum Industry*; Cambridge University Press: Cambridge, UK, 2000.

- (3) Farn, R. J. *Chemistry and Technology of Surfactants*; Blackwell Publishers: Oxford, UK, 2006.
- (4) Christian, S. D.; Scamehorn, J. F. *Solubilization in Surfactant Aggregates*; Surfactant Science Series Vol. 55; Marcel Dekker Inc.: New York, 1995.
- (5) Baeurle, S. A.; Kroener, J. J. *Math. Chem.* **2004**, *36*, 409–421.
- (6) Moroi, Y. *Micelles: Theoretical and Applied Aspects*; Plenum Press: New York, 1992.
- (7) van Os, N. M., Ed. *Nonionic Surfactants: Organic Chemistry*; Surfactant Science Series Vol. 72; Marcel Dekker Inc.: New York, 1998.
- (8) Cutler, W. G.; Kissa, E. *Detergency: Theory and Technology*; Surfactant Science Series Vol. 20; Marcel Dekker Inc.: New York, 1987.
- (9) Lai, K.-Y. *Liquid Detergents*; Surfactant Science Series Vol. 67; Marcel Dekker Inc.: New York, 1997.
- (10) Mittal, K. L. *J. Pharm. Sci.* **2006**, *61*, 1334–1335.
- (11) Meadows, J.; Phillips, G. O.; Williams, P. A. *Carbohydr. Polym.* **1990**, *12*, 443–459.
- (12) Wang, S. T.; Hansen, P. M. T.; Barringer, S. A. *Food Hydrocolloids* **1998**, *12*, 115–119.
- (13) Pancera, S. M.; Itri, R.; Petri, D. F. S. *Macromol. Biosci.* **2005**, *5*, 331–336.
- (14) Söderman, O.; Stilbs, P.; Price, W. S. *Concepts Magn. Reson., Part A* **2004**, *24A*, 121–135.
- (15) Akhter, M. S.; Al-Alawi, S. M. *Colloids Surf., A* **2000**, *164*, 247–255.
- (16) Ko, Y. C. *Bull. Korean Chem. Soc.* **2007**, *28*, 1857–1859.
- (17) Nozaki, Y.; Schechter, N. M.; Reynolds, J. A.; Tanford, C. *Biochemistry* **1976**, *15*, 3884–3890.
- (18) Xu, R.; Winnik, M. A.; Hallett, F. R.; Riess, G.; Croucher, M. D. *Macromolecules* **1991**, *24*, 87–93.
- (19) Cocera, M.; Lopez, O.; Estelrich, J.; Parra, J. L.; de la Maza, A. *Chem. Phys. Lipids* **2001**, *110*, 19–26.
- (20) Lagerberg, J. W.; Van Steveninck, J.; Dubbelman, T. M. *Photochem. Photobiol.* **1998**, *67*, 729–733.
- (21) Mohr, A.; Talbiersky, P.; Korth, H.-G.; Sustmann, R.; Boese, R.; Bläser, D.; Rehage, H. *J. Phys. Chem. B* **2007**, *111*, 12985–12992.
- (22) Aguiar, J.; Carpena, P.; Molina-Bolivar, J. A.; Carnero-Ruiz, C. *J. Colloid Interface Sci.* **2003**, *258*, 116–122.
- (23) Ross, S.; Olivier, J. P. *J. Phys. Chem.* **1959**, *63*, 1671–1674.
- (24) Nemethy, G.; Ray, A. *J. Phys. Chem.* **1971**, *75*, 804–808.
- (25) Herrmann, C. U.; Kahlweit, M. *J. Phys. Chem.* **1980**, *84*, 1536–1546.
- (26) Regev, O.; Zana, R. *Colloid Interface Sci.* **1999**, *210*, 8–17.
- (27) Funasaki, N.; Hada, S.; Neya, S. *Chem. Soc. Jpn.* **1989**, *62*, 1725–1730.
- (28) Jha, R.; Ahluwalia, J. C. *J. Phys. Chem.* **1991**, *95*, 7782–7784.
- (29) Biaselle, C. J.; Millar, D. B. *Biophys. Chem.* **1975**, *3*, 555–559.
- (30) Tummino, P. J.; Gafni, A. *Biophys. J.* **1993**, *65*, 1580–1582.
- (31) Hara, K.; Suzuki, H.; Takisawa, N. *J. Phys. Chem.* **1989**, *93*, 3710–3713.
- (32) Kato, M.; Ozawa, S.; Hayashi, R. *Lipids* **1997**, *32*, 1229–1230.
- (33) Lesemann, M.; Thirumoorthy, K.; Kim, Y. J.; Jonas, J.; Paulaitis, M. E. *Langmuir* **1998**, *14*, 5339–5341.
- (34) Baden, N.; Kajimoto, O.; Hara, K. *J. Phys. Chem. B* **2002**, *106*, 8621–8624.
- (35) Benniston, A. C.; Harriman, A. *J. Chem. Soc., Faraday Trans.* **1994**, *90*, 2627–2634.
- (36) Baden, N.; Kajimoto, O.; Hara, K. *J. Phys. Chem. B* **2002**, *106*, 8621–8624.
- (37) Alamiry, M. A. H.; Benniston, A. C.; Copley, G.; Elliott, K. J.; Harriman, A.; Stewart, B.; Zhi, Y. G. *Chem. Mater.* **2008**, *20*, 4024–4032.
- (38) Strickler, S. J.; Berg, R. A. *J. Chem. Phys.* **1962**, *37*, 814–822.
- (39) Takiguchi, Y.; Uematsu, M. *J. Chem. Thermodyn.* **1996**, *28*, 7–16.
- (40) Eggert, J. H.; Xu, L.-W.; Che, R.-Z.; Chen, L.-C.; Wang, J.-F. *J. Appl. Phys.* **1992**, *72*, 2453–2461.
- (41) Born, M.; Wolf, E. *Principles of Optics: Electromagnetic Theory of Propagation, Interference and Diffraction of Light*, 7th ed.; Cambridge University Press: Cambridge, UK, 1999.
- (42) Dodin, G.; Aubard, J.; Falque, D. *J. Phys. Chem.* **1987**, *91*, 1166–1172.
- (43) Georges, J. *Spectrochim. Acta, Part A* **1995**, *51*, 985–994.
- (44) Kasha, M. *Radiat. Res.* **1963**, *20*, 55–71.
- (45) Yassar, A.; Horowitz, G.; Valat, P.; Wintgens, V.; Hmyene, M.; Deloffe, F.; Srivastava, P.; Lang, P.; Garnier, F. *J. Phys. Chem.* **1995**, *99*, 9155–9159.
- (46) Kong, Y. *Biophys. Chem.* **2002**, *95*, 1–6.
- (47) Smith, J. C.; Graves, J. W.; Williamson, M. *Arch. Biochem. Biophys.* **1984**, *231*, 430–436.
- (48) Biaselle, C. J.; Miller, D. B. *Biophys. Chem.* **1975**, *3*, 355–361.
- (49) Floriano, W. S.; Nascimento, M. A. C. *Braz. J. Phys.* **2004**, *34*, 38–41.
- (50) Harriman, A. *J. Photochem. Photobiol., A* **1992**, *65*, 79–93.
- (51) Watkins, R. C. *Phys. Technol.* **1984**, *15*, 321–328.
- (52) Kauzmann, W. *Adv. Protein Chem.* **1959**, *14*, 1–7.
- (53) Kaneshina, S. *Colloids Surf.* **1985**, *13*, 249–256.
- (54) Hara, K.; Kuwabara, H.; Kajimoto, O.; Bhattacharyya, K. *J. Photochem. Photobiol., A* **1999**, *124*, 159–162.
- (55) Streletsky, K.; Phillis, G. D. *J. Langmuir* **1995**, *11*, 42–47.
- (56) Giddings, L. D.; Olesik, S. V. *Langmuir* **1994**, *10*, 2877–2883.
- (57) Kaneshina, S.; Kamaya, H.; Ueda, I. *Biochim. Biophys. Acta* **1982**, *685*, 307–314.